PASSIVE VENTILATION FLOW CONTROL FOR AIRCRAFT GUST LOAD ALLEVIATION

Yasuhiro Tani*, Shuhei Seki*, Shigeru Aso*
***Department of Aeronautics and Astronautics, Kyushu University, Japan**

Keywords: *Gust load alleviation, wing, aerodynamics, wind tunnel test*

Abstract

To reduce the gust load of aircraft wings, a new gust load alleviation method using passive ventilation concept with porous surface and deflectable vanes has been proposed. To confirm the effect of this concept, low speed wind tunnel test was conducted on the wing models with gust load alleviation mechanisms. To measure the gust response aerodynamic forces, a gust generator was installed to a low speed wind tunnel in Kyushu University. Three component aerodynamic forces were measured for the steady flow and unsteady gust flow conditions, and it was confirmed that the proposed concept provides the reduction of gust load for aircraft wings with simple mechanism.

1 Introduction

Aircraft safety is one of the most important problem to be solved for the air transport systems. Considering the results of aircraft accident analysis, about half of the accidents are caused by the weather or atmospheric conditions [1]. Therefore, some kind of further countermeasures are necessary for the gust and rapid wind change conditions to reduce the aircraft accidents. In this study, we focused on the gust load alleviation (GLA) for the aircraft wings. Various concepts have been investigated for GLA by many researchers and some techniques have been applied to the actual aircrafts [2]. GLA methods are categorized into two types; active method and passive one. In typical active method, the flow disturbances or aircraft motion are detected by some sensors, then the control surfaces are deflected by the actuators [3]. Although the active methods are effective, they have disadvantages in cost and weight, and it is difficult to apply to small aircrafts. As compared with the active one, passive methods do not require sensors, electric devices or actuators. Therefore, they have advantages in cost and weight, and is applicable to small aircrafts [4-7]. As for the transonic wing, one of the authors have investigated the passive flow control methods using the pressure difference on the wing surface to improve the aerodynamic characteristics. In this method, the internal airflow is generated by the slits or porous surfaces and the flow duct inside of the wing [8-10].

In the authors' previous study, this passive ventilation techniques with surface vanes was applied to the passive gust load alleviation, and showed the effectiveness of reduction of gust load experimentally [11-14]. In this paper, we propose a new passive gust load alleviation concept using porous surfaces and measured unsteady aerodynamic characteristics in the gust wind tunnel test to confirm the effectiveness of this concept.

2 Passive gust load alleviation concept

Fig. 1 shows the basic concept of the gust load alleviation mechanism using the passive ventilation. The ventilation mechanism consists of porous surfaces on the upper and the lower surfaces of the wing and the internal flow duct between the surfaces. Increasing of the pressure difference between the upper and the lower surfaces caused by the upward gust flow generates the internal flow from the lower to the upper surface. This internal flow decreased the pressure difference between the surfaces, and it causes the reduction of the lift increase.

Deflectable vanes are also considered to suppress the internal flow in steady flow condition.

(a) solid wing (b) porous surface wing

Fig. 1. Basic concept of passive gust load alleviation with passive ventilation mechanism.

3 Experimental Methods

3.1 Wind Tunnel Test Facility

Wind tunnel test was conducted in a small low-speed wind tunnel at department of aeronautics and astronautics, Kyushu University, shown in Fig. 2. This wind tunnel is open-jet type and its test section size is 300 mm x 300 mm, with maximum speed of 30 m/s. In this study, we installed a gust generator in the two dimensional test section cart. The gust generator has two blades of 80 mm chord length and 296 mm span and was set at 150 mm upstream of the test wing model leading edge, shown in Fig. 3. The gust generator was controlled by a microcomputer, oscillating two blades using a servo-motor, to generate arbitrary gust flow patterns.

(a) Two dimensional test section.

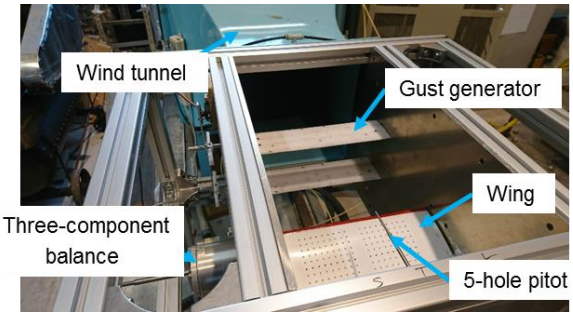

(b) Setup of the gust generator and the test wing model.

Fig. 2. Small low speed wind tunnel in Kyushu University.

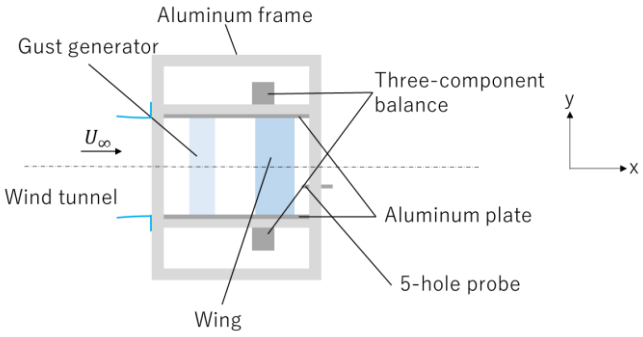

(a) Plan view

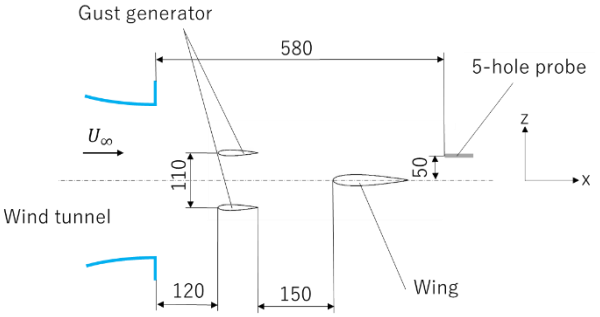

(b) Side view

Fig. 3. Layout in wind tunnel test section.

3.2 Test Models

Two types of wind tunnel test models were prepared as the passive ventilation gust load alleviation wing.

One is a Model-A used for test case-A, shown in Fig. 4. Span and chord length of this model is 296 mm and 150 mm respectively, whose airfoil section is NACA0015. Three exchangeable surface skins were prepared for both the upper and the lower surfaces; a porous surface skin with 324 holes of 1 mm diameter in 10 mm spacing, a porous surface skin with 2.5 mm diameters holes, and a solid surface skin without holes. The holes are distributed from 17%c to 70%c location. Four inner deflectable vanes are installed inside the model. The vanes are made of 0.3 mm thick plastic plate with C-shaped cutting lines as vanes.

Another is a Model-B with porous holes which is distributed near the leading edge, shown in Fig. 5, and was used for test case-B and case-C. The porous holes are 1 mm diameter with 3 mm spacing, located from 4%c to 24%c on upper and lower surfaces. Four rigid deflectable vanes with hinges are installed inside the model. Thin

plastic adhesive tapes were used to cover the porous holes to change the porous distribution.

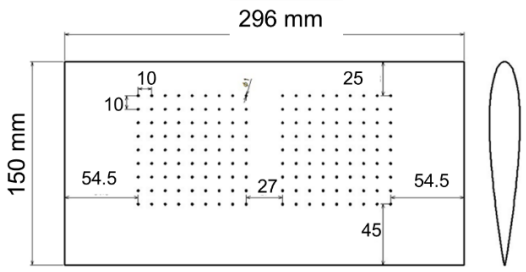

(a) Dimensions of Model-A

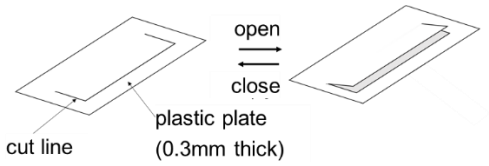

(b) Deflectable inner vane of Model-A

(c) Base configuration (solid surfaces)

(d) Passive Ventilation, ϕ = 1 mm

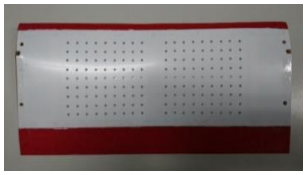

(e) Passive Ventilation, ϕ = 2.5 mm

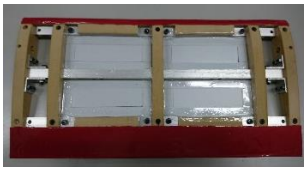

(f) Inner structure with deflectable vanes

Fig. 4. Passive ventilation wing, Model-A.

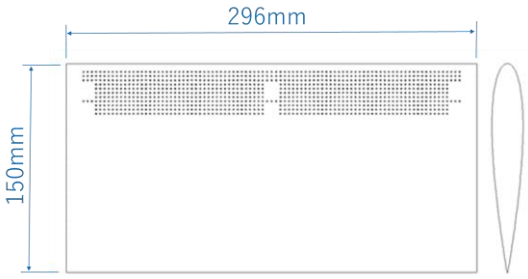

(a) Dimensions of Model-B

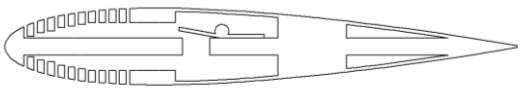

(b) Cross section

(c) Photograph of Model B

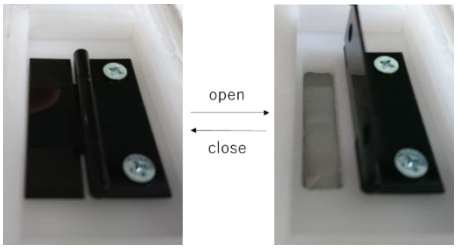

(d) Deflectable inner vane

Fig. 5. Passive ventilation wing, Model-B.

3.3 Measurement System

Three component aerodynamic forces and moment were measured using a pair of side-wall force balances (Nissho electric works, LMC-3531-5) mounted on both sidewalls of the test section, and the wing model was mounted on the force balances. Flow velocity were measured using a five-hole pitot tube (Aeroprobe Corporation, P-C05C03S-S-SX-S-152, 3.18 mm diameter) and pressure sensors (ALLSENSORS, 5INCH-D-4V). The five-hole pitot tube was set at upward of the wing model for the gust flow monitoring during the test.

3.4 Test Cases

Flow velocity was set as 25 m/s, and the angle of attack was ranged from -6 to 20 degrees for case-A and from 0 to 10 degrees for case-B. Reynolds number is 2.48 x 10^5 based on the wing chord length. In this study, gust flow pattern was set as half cycle of sinusoidal, shown in Fig. 6, changing the maximum vertical velocity U_{gust} and frequency f of sinusoidal flow pattern.

Schematic sketch of the passive ventilation configuration tested are shown in Fig. 7 and 8. For the test case-A, two configurations were tested in steady and gust flow conditions. "Base configuration" is a solid wing without passive ventilation mechanism, "PVA configuration" has

porous surface skins and inner vane mechanism. Its porous area was set from 17%c to 70%c on both sides and its diameter was 2.5 mm.

For the test case-B, "Base configuration" with solid surfaces and "PV1 configuration" with porous surface skins between 4%c and 16%c. For the test case-C, four configuration were tested; "Base configuration" with solid surfaces, "PV2 configuration" with porous surface between 4%c and 8%c on both sides, "PV3 configuration" with porous surface between 4%c and 8%c on the upper and between 4%c and 6%c on the lower surface, and "PV4 configuration" with porous surface between 4%c and 8%c on the upper and 4%c on the lower surface.

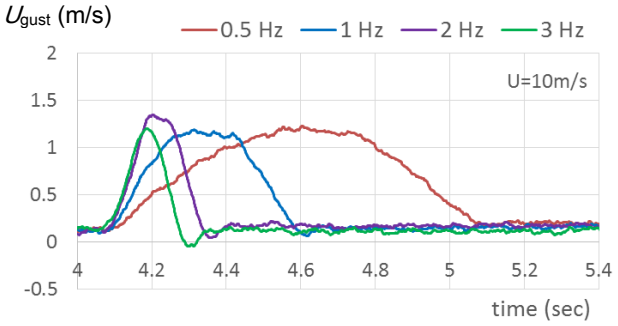

Fig. 6. Example of gust flow pattern: half sinusoidal.

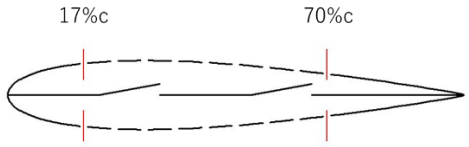

Fig. 7. Test configuration, PVA : Model-A.

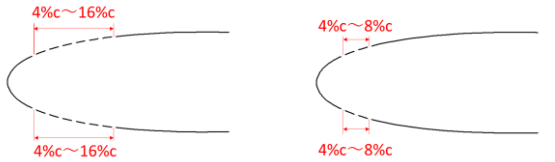

(a) PV1 configuration (b) PV2 configuration

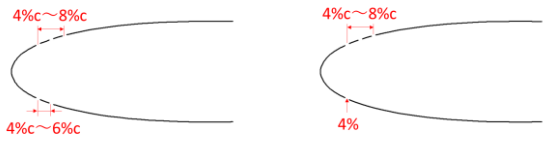

(c) PV3 configuration (d) PV4 configuration

Fig. 8. Test configurations of Model -B.

4 Results and Discussions

4.1 Case-A: the effect of passive ventilation

To examine the effect of the internal flow caused by the passive ventilation, aerodynamic forces were measured in steady flow conditions, and the comparison of Base and PVA configurations is shown in Fig. 9. PVA configuration shows the lower lift coefficient at high angle of attack than Base configuration. This results suggest the effect of decrement of pressure difference between the upper and the lower surfaces caused by the internal flow, and the possibility of passive ventilation concept for gust load alleviation.

Fig. 10 shows the comparison of the lift coefficient in gust flow at α = 4 and 8 degrees. Gust flow velocity is 1.5 m/s in 1 Hz frequency. Black line shows that C_L increment by the gust flow of Base configuration is about 0.25, and red line shows that it is about 0.2 of C_L increment for PVA configuration. This means the lift increment by the gust is reduced 20 % by this simple passive ventilation mechanism. Lift coefficient changes are summarized in Fig. 11 for α = 0 to 12 degrees for the gust flow velocity is 1.5 m/s and 1 Hz frequency. Lift change caused by the gust was decreased by the passive ventilation for steady lift coefficient at the range of 0.2 to 0.5. The effect of the passive ventilation is small for the low angle attack conditions because the pressure difference between the upper and the lower surface is small. From this result, C_L changes are decreased by the passive ventilation PVA configuration in wide range of gust velocity and frequency conditions, and is confirmed the effectiveness for gust load alleviation with simple mechanism.

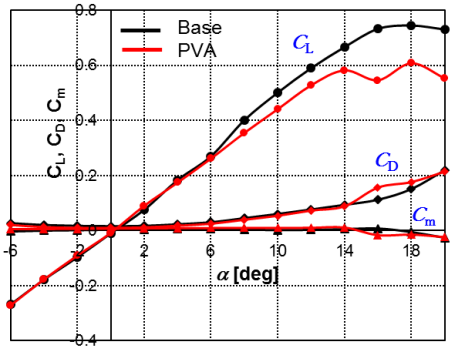

Fig. 9. Comparison of C_L, C_D, and C_m of Case-A in steady flow.

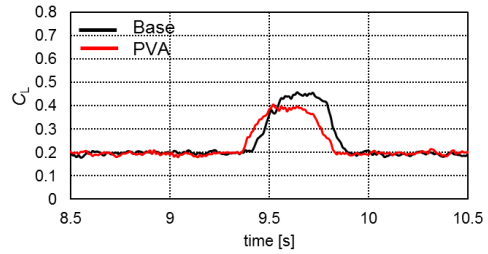

(a) α = 4 degree

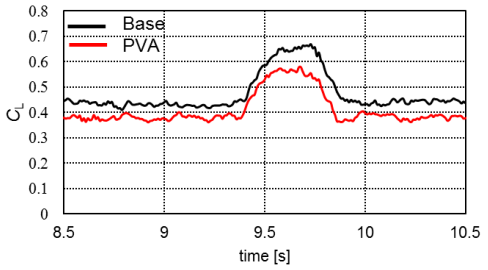

(b) α = 8 degree

Fig. 10. Comparison of C_L time history in gust flow, (Case-A, U_{gust} = 1.5 m/s , f = 1 Hz).

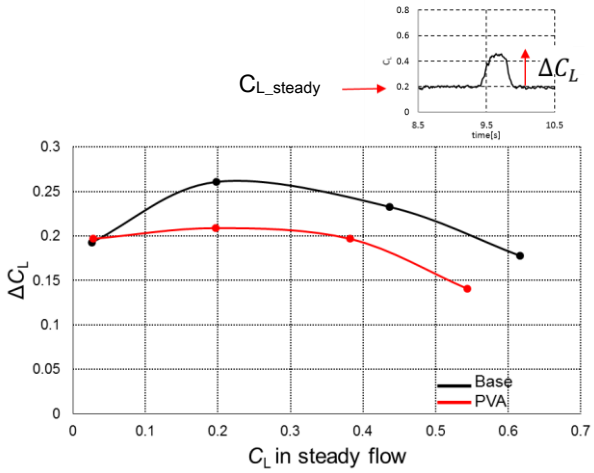

Figure 11. Effect of C_L change in gust flow, (Case-A, U_{gust} = 1.5 m/s, f = 1 Hz).

4.2 Case-B: the effect of forward distributed porous surface

Considering the application of this concept to the aircraft and the reduction of drag increment, the area of porous surface should be small. Furthermore, the porous area near the leading edge of the wing could obtain larger internal flow with small porous area, because of the large pressure difference between upper and lower surfaces. Therefore, wind tunnel test using Model-B with forward distributed porous surface were carried out for PV1 configuration.

Fig. 12 shows the the comparison of three component forces in steady flow condition. Comparing to the Base configuration, PV1 configuration shows the lift decrement caused by the internal flow from the lower surface to the upper surface. These results show that even small porous surface area near the leading edge is effective as a passive ventilation flow mechanism. However, maximum lift coefficient of PV1 configuration is smaller than that of Base configuration. Therefore, further consideration is needed to minimize the lift decrease in steady flow.

Fig. 13 shows the comparison of the lift coefficient during gust flow at α = 4 degrees. Gust vertical flow velocity U_{gust} was 1.5 m/s and its frequency f = 0.5 to 4 Hz. Black line shows that C_L increment by the gust flow for Base configuration and red line for PV1 configuration. C_L increment of PV1 configuration is smaller than that of Base configuration. This means that small area of porous region near the leading edge is effective to reduce the gust load.

Fig. 14 shows the comparison of lift coefficient change for Base and PV1 configurations. Gust flow condition is 1.5 m/s gust vertical flow velocity and frequency from 0.5 to 4 Hz. Horizontal axis shows C_L in steady flow and vertical axis shows the C_L change caused by the gust flow. PV1 configuration shows smaller lift increment by the gust flow than that of Base configuration in all the measured conditions.

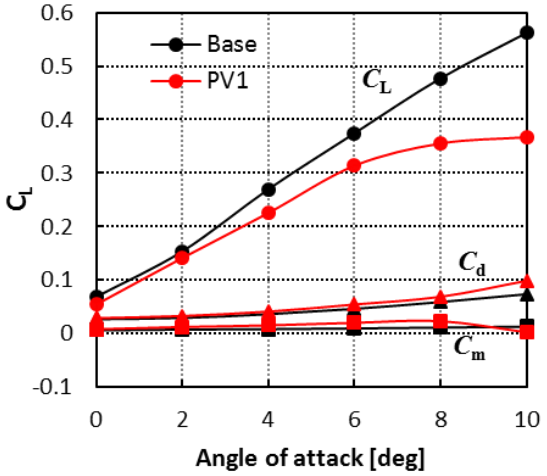

Fig. 12. Comparison of C_L, C_D, and C_m of PV1 in steady flow (Case-B).

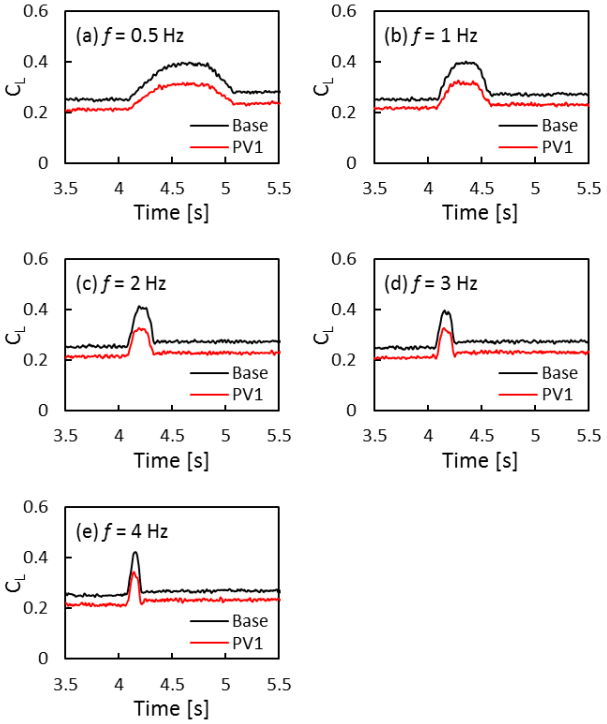

Fig. 13. Comparison of C_L time in gust flow (Case-B, α = 4 deg, U_{gust}=1.5 m/s).

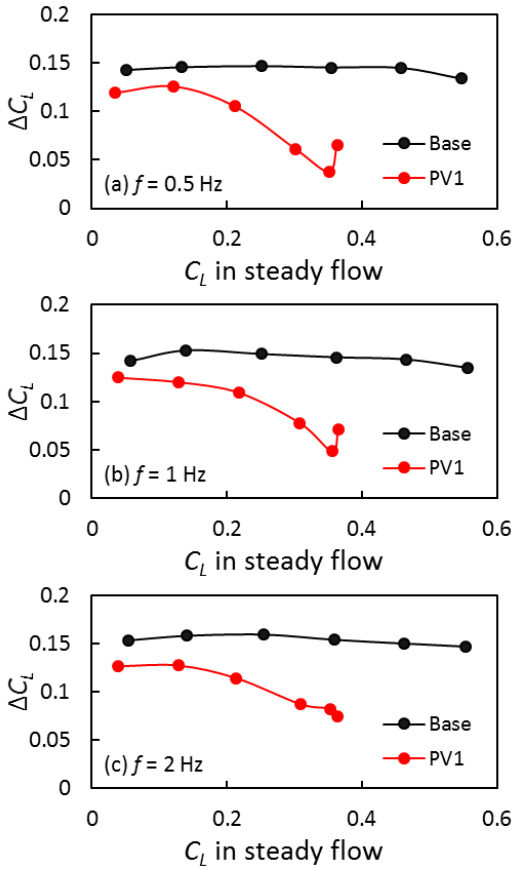

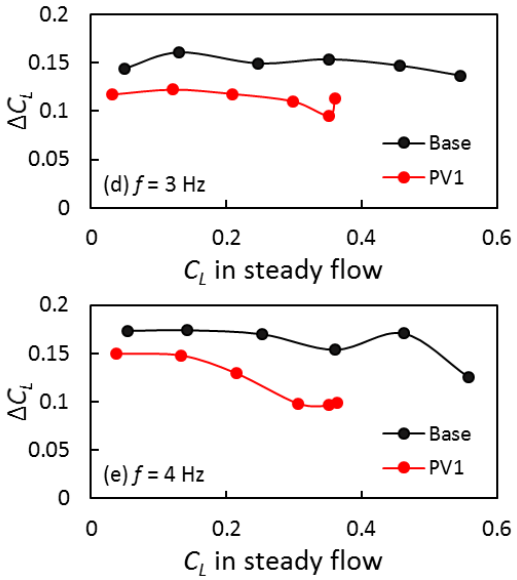

Fig. 14. Comparison of ΔC_L in gust flow (Case-B, U_{gust}=1.5 m/s).

4.3 Case-C: the effect of porous area on lower surface

To examine the effect of the porous area on the lower surface, PV2, PV3 and PV4 configurations were compared with Base configuration.

Fig. 15 shows the comparison of C_L in steady flow condition. PV2 configuration shows the smallest C_L than other configurations. C_L decreases with increasing porous area on the lower surface. However, stall angle of attack does not change by the porous area. Fig. 16 shows the time history data of C_L at α = 8 deg for f = 1 and 3 Hz. The data in this figure show that all the passive ventilation configurations show the smaller C_L increase caused by the gust flow than Base configuration. Fig. 17 shows the comparison of ΔC_L to steady C_L for all the configurations at α = 0 to 20 degrees. The figures show that the passive ventilation configurations can reduce the gust load at the lower angle of attack than stall. In this figure, PV2 and PV3 configurations show ΔC_L peak at α = 12 deg. It is considered that this is caused by the rapid increase of C_L by the massive flow separation during the gust.

Fig. 18 shows the comparison of C_{Lmax} in steady flow and ΔC_L by the gust at C_L =0.3. C_L increase by the gust decreases with increasing porous area, but C_{Lmax} in steady flow decreases at the same time. Because the gust load

alleviation mechanism in this study is essentially passive, the internal flow occurs when the pressure difference exists between upper and lower surfaces, especially at high angle of attack. Therefore, additional work is required for the suppression of the internal flow in steady flow condition, but it is hoped that this passive ventilation mechanism will help in reducing the gust load for the aircraft wing.

5 Conclusions

The effectiveness of the passive ventilation on gust load alleviation has been investigated by low speed wind tunnel experiments. The conclusions are summarized as follows;

1) Passive ventilation wing with porous surface skin and inner deflectable vane mechanisms alleviates the gust load by the internal flow caused by the pressure difference between upper and lower surfaces.

2) Porous region near the leading edge is sufficient to reduce the gust load. However, additional work is required to optimize the porous distribution and internal vane mechanism.

Acknowledgement

This work was supported by JSPS KAKENHI Grant Number (JP16K06887). The authors would like to thank Mr. Kazuhiko Morishita, technical staff of the Department of Aeronautics and Astronautics in Kyushu University, for his technical support on wind tunnel test.

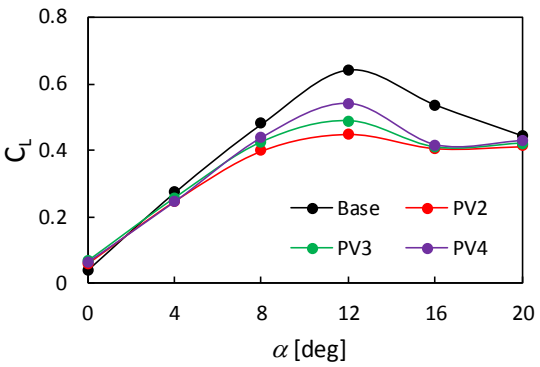

Fig. 15. Comparison of C_L of Case-C in steady flow.

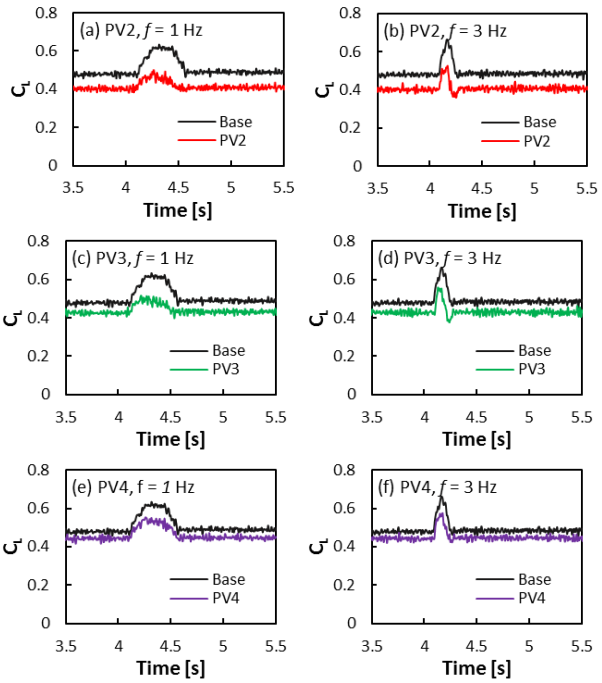

Fig.16. Comparison of C_L time history in gust flow (Case-C, α = 8 deg, U_{gust}=1 m/s).

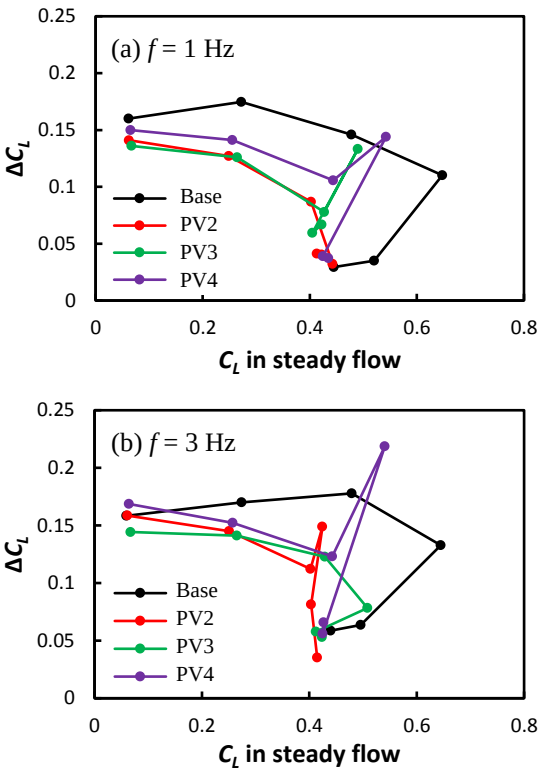

Fig. 17. Comparison of ΔC_L in gust flow (Case-C, U_{gust}=1 m/s).

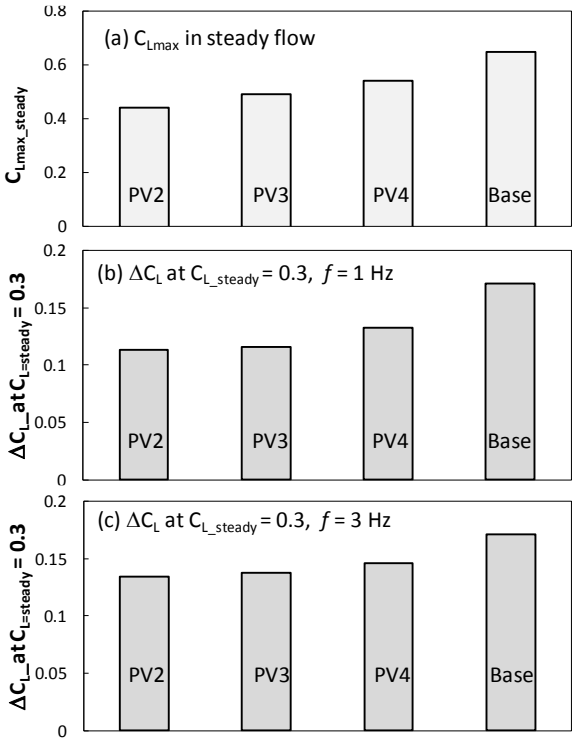

Fig. 18. Comparison of ΔC_L and C_{Lmax} (Case-C, U_{gust} = 1 m/s).

References

[1] Japan transport safety board. JTSB Annual Report 2012 - JTSB Annual Report 2017. 2017.

[2] Active control systems for load alleviation, flutter suppression and ride control. AGARD-AG-175, 1974.

[3] Inokuchi H, et.al. Development of a long range airborne doppler LIDAR. ICAS 2010-10.4.3, 2010.

[4] Guo S, et.al. Gust alleviation of a large aircraft with a passive twist wingtip. Aerospace 2015, pp.135-154, 2015.

[5] Miller S, et.al. Development of an adaptive wing tip device. 50th AIAA/ASME/ASCE/AHS/ASC Structures, Structural Dynamics, and Materials Conference, AIAA 2009-2121, 2009.

[6] Castrichini A. Nonlinear folding wing-tips for gust loads alleviation. AIAA SciTech 56th AIAA/ASCE/ AHS/ASC Structures, Structural Dynamics, and Materials Conference, 2015.

[7] Arrieta A F. Passive load alleviation aerofoil concept with variable stiffness. Composite Structures 116 (2014) 235–242, Sep. 2014.

[8] Kamo K, Tani Y and Amano K. Navier-Stokes simulation of transonic flow around ventilated airfoils. NAL SP-9, pp.133-140, 1988.

[9] Tani Y, Tanaka K, Amano K, et.al. Experimental and numerical analysis on ventilated airfoils. AIAA-91-3335, 1991.

[10] Tani Y and Aso S. A study on improvement of lift-drag characteristics of transonic airfoil with passive ventilation. Memories of Faculty of Engineering, Kyushu University, Vol. 64, No. 1, March 2004.

[11] Tani Y, Hirayama T, Seki S and Aso S. Passive ventilation wing for gust load alleviation. 54th Aircraft Symposium, 1D03, 2016.

[12] Tani Y, Seki S, Hirayama T and Aso S. A research on passive ventilation wing for gust load alleviation. 58th JSASS Annual Meeting, 1D20, 2017.

[13] Seki S, Tani Y and Aso S. Porous wing for passive ventilation gust load alleviation. 55th Aircraft Symposium, 3D04, 2017.

[14] Tani Y, Seki S and Aso S. An experimental study on gust load alleviation using passive ventilation wing concept. AIAA Aerospace Science Meeting, AIAA-2018-1794, 2018.

Contact Author Email Address

mailto:tani@aero.kyushu-u.ac.jp

Copyright Statement